Revista Ciência Agronômica, v. 55, e20228335, 2024
Centro de Ciências Agrárias - Universidade Federal do Ceará, Fortaleza, CE
www.ccarevista.ufc.br

*Scientific Article*
ISSN 1806-6690

# Artificial neural networks for predicting backwashing in screen filters for irrigation[1]

**Mádilo Lages Vieira Passos[2], Alan Bernard Oliveira de Sousa[3]*, Adunias dos Santos Teixeira[3], Carlos Wagner Oliveira[4]**

**ABSTRACT** - Careful implementation of a filtration system is essential for maintaining the operation of an irrigation system. Failure to maintain a filtration system can have a negative effect on irrigation pressure and uniformity. To avoid this problem, it is important to clean the filters, which can be done either manually or automatically. Predicting the correct time to clean the filters helps maintain the pressure and efficiency of the system. The aim of this study was to model backwash pressure as a function of water quality and the filter inlet pressure load using artificial neural networks. The characteristics of the water were determined using sensors to measure the pH (hydrogen potential), turbidity, total dissolved solids (TDS), and temperature. A pressure transducer was used to quantify the drop in pressure and the need to clean the filters. To predict the need for cleaning the irrigation filters, a hydraulic structure was constructed that included a screen filtration system with a mesh size of 120, cleaned by backwashing. The need for cleaning estimated by the multilayer perceptron feedforward artificial neural networks with 2-4-1 architecture performed well in modelling the temporal evolution of the pressure load in the screen filtration system (120 mesh), whereas adjusting the pressure load based on the water quality characteristics (pH, turbidity, total dissolved solids and temperature) performed poorly.

**Key words:** Computational Intelligence. Multilayer Perceptron. Pressure Load.

DOI: 10.5935/1806-6690.20240035
Editor-in-Article: Prof. Alek Sandro Dutra - alekdutra@ufc.br
*Author for correspondence
Received for publication on 20/01/2022; approved on 03/10/2023
[1]Extracted from the dissertation of the lead author presented to the Postgraduate Program in Agricultural Engineering of the Universidade Federal do Ceará, Fortaleza, Ceará
[2]Department of Agricultural Engineering, Universidade Federal de Lavras (UFLA), Lavras-MG, Brazil, madilolages@hotmail.com (ORCID ID 0000-0003-2495-1612)
[3]Department of Agricultural Engineering, Universidade Federal do Ceara (UFC), Fortaleza-CE, Brazil, alan.sousa@ufc.br (ORCID ID 0000-0001-7786-0306), adunias@ufc.br (ORCID ID 0000-0002-1480-0944)
[4]Centre for Agricultural Science and Biodiverity, Universidade Federal do Cariri (UFCA), Crato-CE, Brasil, carlos.oliveira@ufca.edu.br (ORCID ID 0000-0003-1013-2974)

## INTRODUCTION

The quality of the irrigation water can decide the type of crop and the irrigation method to be used (AYERS; WESTCOT, 1991). In irrigation systems, the main problem is clogging of the filters and emitters, especially when low-quality water is used, since this can contain high concentrations of dissolved and suspended solids (ELBANA; CARTAGENA; PUIG-BARGUÉS, 2012).

To remove suspended particles, the screen filter is most commonly used due to its ease of handling and low cost (WU *et al*., 2014; ZONG *et al*., 2015). However, this type of filter can quickly become clogged, and requires constant cleaning. Filter clogging impairs the flow of water and its distribution throughout the irrigation system, and can affect its hydraulic performance (MESQUITA; TESTEZLAF; RAMIREZ, 2012; RIBEIRO *et al*., 2008). In this respect, cleaning the filter element is essential for the system to function.

Filters can be cleaned manually or by backwashing. Backwashing involves reversing the flow of water through the filter, i.e. from the inside to the outside of the filter (ZONG *et al*., 2019). Backwashing can be automatic: for this process, the system is equipped with a device that detects the difference in internal pressure of the filter. Upon reaching a preset value, the control device sends a signal that activates the valves and initiates cleaning (DURAN-ROS *et al*., 2009). According to Jianhua *et al*. (2019), hydraulically operated self-cleaning screen filters have better water flow capacity, a stronger cleaning effect, and a longer working life.

Backwashing can also be set by monitoring the time, i.e. when filtration reaches a pre-set period, the system automatically begins the cleaning process (ZAKI *et al*., 2021). The period depends on the quality of the water, the rate of filtration, and the filter layer (ADIN; ALON, 1986; TESTEZLAF, 2008).

Therefore, by monitoring water quality, flow parameters under pressure, and the construction characteristics of the filter element, it is possible to model the pressure and help define optimum maintenance levels. In this respect, inference using computer algorithms, such as artificial neural networks, can be satisfactory. The architecture of these networks varies in terms of the number of layers and input parameters and how the connections between them are made, allowing them to be used in a variety of situations (FATHA; MADANIFARB; ABBASIA, 2020; HEMMAT ESFE *et al*., 2015; LEE; LEE; YOON, 2019).

Using neural networks, it is possible to predict the best time to carry out backwashing based on monitoring the water quality and the pressure loss in the filters. The aim of this study was therefore to model backwash pressure as a function of water quality and filter inlet pressure using artificial neural networks.

## MATERIAL AND METHODS

The experiment was conducted at the Hydraulics and Irrigation Laboratory of the Federal University of Ceará (UFC) in Fortaleza, Ceará.

### Hydraulic structure and water quality

The hydraulic structure built to evaluate the filtration system can be seen in Figure 1.

The system consisted of pipes with a diameter of 32 mm, a 120 mesh (1”) screen filter, a 120 mesh (1”) disc filter, and two modes of operation: filtration and backwashing. When filtering, the flow was via the screen filter. During the automatic cleaning process, the filtration flow was via the disc filter, with the flow direction reversed in the screen filter.

The operating modes of the system were regulated by five electric valves (1” HV 24.0 Vac RainBird). For this, a control module was assembled (Figure 2) comprising a 5A 12+12 Vac transformer, a 3-channel 5v 10a relay module, and a rocker switch.

The structure was mounted on a hydraulic system with cyclic water reuse. It consisted of a 3 hp motor pump, a rectangular channel together with a Parshall flume, and a 512 L reservoir. The water collected from the reservoir was fed back into the hydraulic structure via the filter and returned to the reservoir through the channel via the Parshall meter.

In order to obtain low-quality water, it was decided to increase the organic matter content with earthworm humus in the proportion of 500 g per 264 L of water (1.89 g $L^{-1}$).

**Figure 1** - Diagram of the hydraulic structure for filtration and backwashing, (a) flow inlet, (b) solenoid valve, (c) screen filter, (d) disc filter, (e) pressure outlet, (f) flow outlet, and (g) backwash flow outlet

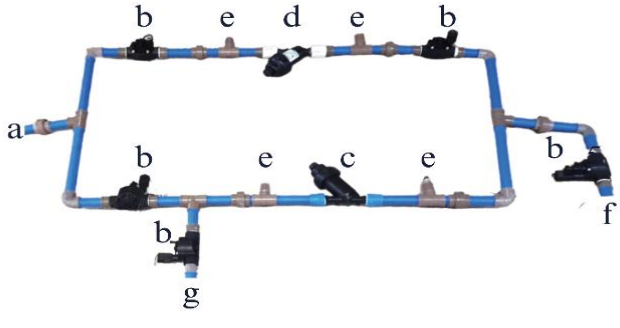

During the filtration tests, the water quality was measured every five seconds using a multiparameter probe based on the Arduino® free hardware and software platform (Figure 3).

The recorded variables were pH, turbidity, total dissolved solids, and temperature. The pH (hydrogen potential) was measured using the Ph4502c sensor module and a probe electrode with a BNC plug. According to the manufacturer, the pH sensor module has the following characteristics: heating voltage of 5 ± 0.2 volts (AC/DC), operating current of 5 to 10 mA, temperature range of 0 ºC to 60 ºC, and analogue output for measurements in the 0.0 to 14.0 pH range.

To quantify the turbidity, the TSW30 turbidity sensor was used. According to the manufacturer, the sensor has the following specifications: voltage of 5 Vdc, maximum current of 30 mA, analogue output of 0 to 4.5 Vdc or digital output (high - 5 V and low - 0 V), and operating temperature of -20 °C to 90 °C. The measurement range is 0.0 to 1000 ± 30 NTU. The total dissolved solids (TDS) sensor operates up to a maximum temperature of 55.0 °C, with an input voltage of from 3.3 to 5.5 V, and analogue signal output of 0 to 2.3 V. The suggested measurement range is between 0.0 and 1000.0 ppm (parts per million), or 0.0 to 1000.0 mg $L^{-1}$. The temperature was recorded using a DS18B20 sensor; this has an operating voltage of 3 to 5.5V, a measurement range of -55 ºC to 125 ºC, accuracy of +/- 0.5 ºC between -10 ºC and 85 ºC, and a 108 cm-long cable.

**Figure 2** - Schematic representation of the solenoid-valve control module for releasing the flow for filtration and/or backwashing, (a) AC source, (b) transformer 12V+12V, (c) relay module, (d) rocker key, (e) DC source, and (f) solenoid valves

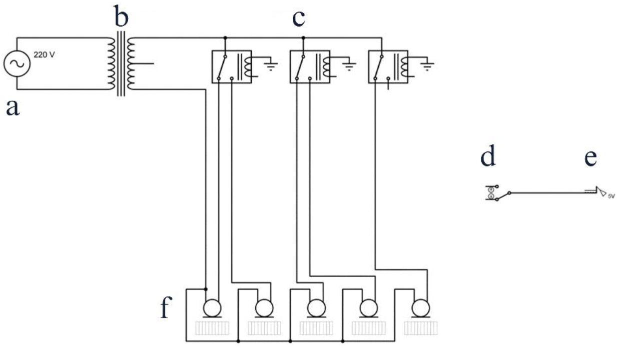


**Figure 3** - Schematic of the multiparameter probe components, (a) Ardunino Nano, (b) HC-06 module, (c) ESP01, (d) voltage regulator, (e) LCD display, (f) 5V bus, (g) GND bus, and (h) three-way terminals

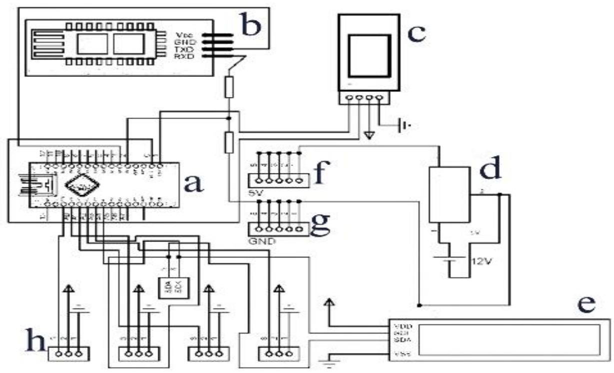


The data was sent to WebService to be viewed in real time on a smartphone.

**Assessing the need for backwashing**

To assess the need for cleaning and then model the drop in pressure, backwashing was applied only to the 120 mesh stainless steel screen filter with a 1” thread.

To define the correct time for backwashing, pressure transducer sensors were installed at the inlet and outlet of the filter coupling. According to the manufacturer, the sensor has the following specifications: operating voltage of 5 Vdc, maximum current of 30 mA, analogue output of 0.5 to 4.5 Vdc, operating temperature of -40 °C to 100 °C, and a burst pressure three times the upper limit. The measuring range is 0.0~0.40 to 6.0 bar.

The drop in pressure is given by the difference between the readings of the two sensors. However, it was found that the manometric pressure at the filter outlet was very close to zero for the flow rates under evaluation, so it was not possible to attribute the variation in values observed in the sensor (based on the lower limit of the measurement range) to the pressure at the edge of the filter. It should be noted that this phenomenon may be associated with the position of the filter flow outlet, which was very close to the filter and open to the atmosphere.

Therefore, pressure monitoring was restricted to the filter inlet. In any case, backwashing was triggered after an increase of 6 mH2O in the pressure as measured at the start of filtration. The filtration flow rate and cleaning flow rate were 1.5, 2.0, 2.5 and 3.0 $m^3$ $h^{-1}$, with the backwashing operation time set to 1.0 minute.

The pressure increase at the filter inlet was recorded for each flow together with the water quality characteristics (pH, turbidity, TDS and temperature) of the reservoir, and sent to WebService on different channels every five seconds. Since the platform records the date the data was added, it was possible to count each period needed to reach the backwash pressure load.

**Calibration of the pressure transducer sensor**

Calibration was carried out on a scale of metres of water column (mH2O) in the range of 0.0 to 30.0 mH2O.

To do this, a structure was built to hold the sensor and a calibrated pressure gauge. The standard pressure gauge had a scale of 0 to 4 kgf $cm^{-2}$ at intervals of 0.02 kgf $cm^{-2}$ and had been previously calibrated at the Mechanical Metrology Laboratory (LAMETRO) of UFC.

Pressures from 0.0 to 3 kgf $cm^{-2}$ (30.0 mH2O) were measured in variations of 0.01 kgf $cm^{-2}$ (1.0 mH2O). Ten repeated values were measured in digital numbers with a resolution of 10 bits (0 to 1023) for any one pressure. WebService was again used to store the data, which was transferred every five seconds. A printed circuit board based on the Arduino Nano platform was built to calibrate the sensor and monitor pressure during the study.

During calibration, the water temperature was recorded by the DS18B20 sensor and the atmospheric pressure, temperature and relative humidity by the BME280 sensor. Ambient air conditions were recorded by a data logger comprising the Arduino Nano, the BME280 sensor, a micro-SD card module, and the RTC DS1307 real time clock.

The simple linear regression model was chosen for the sensor calibration equation. The coefficients were estimated using the ordinary least squares method (OLS). The significance of the regression model was determined using Student's t-test for the angular (b) and linear (a) coefficients at a level of 5%. The following indicators were used to evaluate the statistical performance: root mean square error (RMSE), correlation coefficient (r), coefficient of determination ($R^2$), concordance index (Willmott *et al*., 1985) (d), and the confidence or performance index (c). The confidence index (c) was classified as per Camargo and Sentelhas (1997).

**Cleaning prediction and backwashing**

After carrying out the tests for each flow rate, and obtaining the data set containing the variation in pressure load at the filter inlet over time as well as the water quality characteristics, the multilayer perceptron artificial neural network (MLP) with one hidden layer was trained and validated to predict the need for cleaning (backwashing).

The predictive models were fitted to establish the cleaning time for each filtration flow rate based on the inlet pressure load (dependent variable) and filtration time (independent variable). The adjustment was also made using the water quality characteristics. As such, the independent variable (predicted) was taken to be the pressure at the filter inlet and the accumulated time until this pressure was reached (seconds) plus 4 input variables (independent): pH, turbidity, TDS and temperature. With the exception of temperature, it was decided to use the readings taken by the water quality sensors in units of electrical potential (volt).

The sigmoid logistic activation function was chosen for all the hidden neurons and the linear output. The synaptic weights and activation thresholds (bias) were adjusted using the backpropagation algorithm with a momentum term.

Ten rounds of training/validation were carried out. For the pressure load x time adjustment, the training samples were randomly selected from the set in the proportion of 70% for training and 30% for validation (hold out). In the model for the quality variables, the proportion was 75% for training and 25% for validation. For each group in the 10 rounds, the mean square error (MSE) and coefficient of determination ($R^2$) were used and stored as metrics of statistical performance and inferences of underfitting and overfitting during the training and testing stages. The parameters (weightings) for the best and worst performances were also saved.

## RESULTS AND DISCUSSION

**Descriptive summary of the water quality**

A descriptive summary of the readings in volts taken by the pH, turbidity, total dissolved solids (TDS) and temperature (ºC) sensors can be seen in Table 1.

With the exception of the flow rate of 3.0 $m^3$ $h^{-1}$, the pH and TDS sensors showed the greatest values.

Calibration of the pressure transducer sensor

The linear model fitted to the pressure transducer sensor is shown in Equation 1.

$$\hat{y} = 14.909T - 7.0155 \quad (1)$$

where T is the voltage read by the sensor in volts.

Table 2 shows the t-test results of significance for the angular coefficients (b) and intercepts (a), as well as the performance measurements: root mean square error (RMSE), coefficient of determination ($R^2$), correlation coefficient (r), concordance index (d), and confidence or performance index (c).

**Cleaning prediction and backwashing**

The variation in pressure load at the screen filter inlet is shown in Figure 4.

Fourteen backwashes were carried out at flow rates of 2.0 and 3.0 $m^3$ $h^{-1}$, and 13 at the flow rate of 2.5 $m^3$ $h^{-1}$; the pressure load was returned to the same levels as those seen at the start of filtration for the above flow rates, and the cleaning time was kept practically constant following the backwashes. It can therefore be concluded that the developed flow reversal system was efficient in clearing the screen filter.

At a flow rate of 1.5 $m^3$ $h^{-1}$, only three efficient backwashes were generated, and automatic cleaning was no longer possible (Figure 4A). Duran-Ros *et al*. (2009), working with the automatic cleaning of a screen filter with a diameter of 50.8 mm, and a filtration surface of 1100 $cm^2$ and 120 microns, attributed inefficient backwashing to insufficient pressure, and also reported that increasing the pressure of the filtration system from 300 to 500 kPa increased the percentage of efficient backwashes from 9.31% to 64.16%. Similarly, Salcedo, Testezlaf and Mesquita (2011) associated failures in the backwashing process with the use of incorrect flow rates and cleaning times. Solé-Torres *et al*. (2019) also pointed out that backwashing requires higher pressures than do the other system components.

**Table 1** - Mean values (AVE), minimum values (MIN), maximum values (MAX), coefficient of variation (CV), number of observations (n) for pH, turbidity, total dissolved solids (TDS), and water temperature (Temp) for flow rates of 1.5, 2.0, 2.5 and 3.0 $m^3$ $h^{-1}$

| | Flow rate 1.5 $m^3$ $h^{-1}$ | | | |
|---|---|---|---|---|
| | pH (volt) | Turbidity (volt) | TDS (volt) | Temperature (°C) |
| AVE | 3.409 ± 0.0029 | 3.046 ± 0.0009 | 0.216 ± 0.0008 | 31.28 ± 0.015 |
| MIN | 3.203 | 2.917 | 0.172 | 30.63 |
| MAX | 3.549 | 3.132 | 0.244 | 31.81 |
| CV(%) | 2.02 | 0.69 | 9.72 | 1.13 |
| n | 546 | 546 | 546 | 546 |
| | Flow rate 2.0 $m^3$ $h^{-1}$ | | | |
| AVE | 2.960 ± 0.0023 | 2.837 ± 0.0006 | 0.773 ± 0.0085 | 31.67 ± 0.027 |
| MIN | 2.803 | 2.757 | 0.000 | 30.56 |
| MAX | 3.403 | 2.887 | 0.940 | 32.75 |
| CV(%) | 1.94 | 0.55 | 27.48 | 2.10 |
| n | 623 | 623 | 623 | 623 |
| | Flow rate 2.5 $m^3$ $h^{-1}$ | | | |
| AVE | 3.104 ± 0.0041 | 2.786 ± 0.0044 | 0.569 ± 0.0103 | 33.39 ± 0.022 |
| MIN | 2.908 | 2.031 | 0.050 | 32.44 |
| MAX | 3.521 | 3.032 | 0.895 | 34.69 |
| CV(%) | 3.84 | 4.61 | 52.68 | 19.02 |
| n | 839 | 839 | 839 | 839 |
| | Flow rate 3.0 $m^3$ $h^{-1}$ | | | |
| AVE | 2.590 ± 0.0053 | 2.652 ± 0.0036 | 0.982 ± 0.0002 | 28.90 ± 0.029 |
| MIN | 2.277 | 2.204 | 0.972 | 27.56 |
| MAX | 2.876 | 2.779 | 1.012 | 33.19 |
| CV(%) | 5.26 | 3.50 | 0.61 | 2.65 |
| n | 656 | 656 | 656 | 660 |

**Table 2** - Statistics of the t-test, root mean square error (RMSE), coefficient of determination ($R^2$), correlation coefficient (r), concordance index (d), and confidence or performance index (c)

| Sensor | Student's t statistic | | | | | |
|---|---|---|---|---|---|---|
| | a | | b | | n | |
| | -156.71* | | 530.77* | | 310 | |
| Pressure transducer | Performance statistic | | | | | |
| | RMSE | $R^2$ | r | d | c | Performance |
| | 0.2956 | 0.9989 | 0.9994 | 0.9998 | 0.9992 | Excellent |

*Significant at 5%

**Figure 4** - Screen filter pressure load: (A) flow rate 1.5 $m^3$ $h^{-1}$, (B) flow rate 2.0 $m^3$ $h^{-1}$, (C) flow rate 2.5 $m^3$ $h^{-1}$, and (D) flow rate 3.0 $m^3$ $h^{-1}$

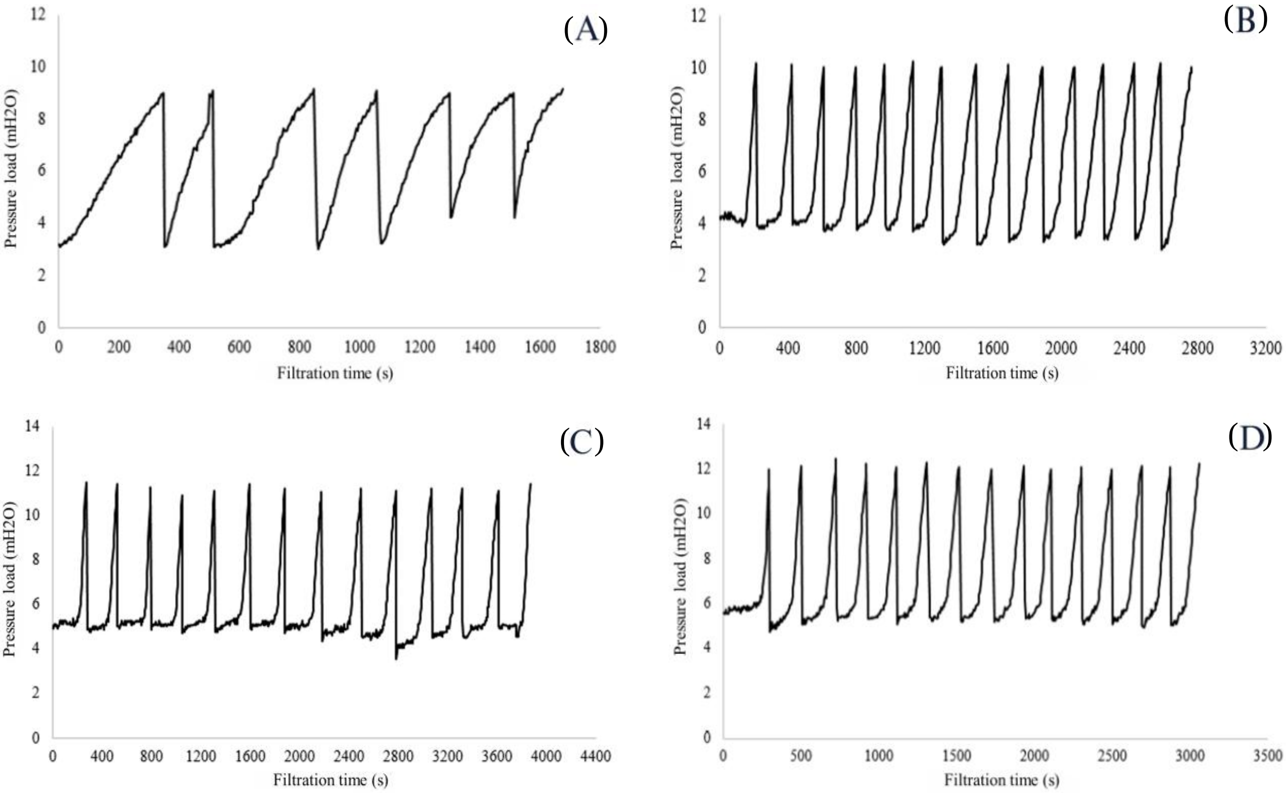


The results of the performance parameters ($R^2$, mean, minimum and maximum) for the filtering time to reach the cleaning pressure load of the screen filter at each flow rate, as determined by the feedforward MLP networks, are shown in Table 3.

The architectures under evaluation had a 2-4-1 configuration, i.e. two neurons in the input layer (time and bias), four in the intermediate layer, and one in the output layer (pressure load). The mean coefficients of determination ($R^2$) during the training stage were greater than 80.00% for each of the flow rates. During the generalisation (validation) stage, they were over 77.00%.

Once the high performance of the models had been verified, the filtration time needed for cleaning was estimated for both high (high MLP) and low (low MLP) accuracy, i.e. using the model weightings generated in one of the ten rounds during the validation stage, corresponding to the highest and lowest observed $R^2$. For comparison purposes, the average of the actual observations was also used as an estimate of the cleaning time, i.e. the cleaning times were recorded, and the average backwashing time was calculated at the end of the test for each flow rate. Table 4 shows the values found, depending on the flow rates and cleaning pressure load.

The cleaning cycle was 380 and 195 seconds at a flow rate of 1.5 and 3.0 $m^3$ $h^{-1}$, respectively. meaning the higher flow rates led to screen clogging. Chi *et al*. (2021) and Mesquita, Testezlaf and Ramirez (2012) pointed out that the drop in pressure is significantly affected by the speed of filtration. Kannan *et al*. (2020) reported that as the flow rate increases, the retained particles and the efficiency of the filter increase, intensifying the drop in pressure and resulting in a greater need for cleaning. If the need for cleaning is high, it is essential to install an automatic backwashing system in order to improve the practicality of the filtration system (KHAN; REHMAN; JAMAL, 2017; RIBEIRO *et al*., 2005).

The time taken to carry out the cleaning cycle using artificial neural networks was only above the average time at the flow rate of 1.5 $m^3$ $h^{-1}$ when considering the set of validations that produced the best-performing network (high MLP). While for the worst set (low MLP), with the exception of the flow rate of 3.0 $m^3$ $h^{-1}$, there was a tendency to overestimate the time relative to the observed average time and that of the high-MLP network. Zong *et al.* (2019) pointed out that setting a long cleaning cycle can lead to a large pressure difference between the inside and outside surface of the screen, with the filter undergoing irreversible deformation, damage to the screen, or incomplete cleaning.

**Table 3** - Performance statistics for the training and validation stages

| Stage | Parameter | Result | | | | Flow rate ($m^3\ h^{-1}$) |
|---|---|---|---|---|---|---|
| | | Mean | Min. | Max. | n* | |
| Training | $R^2$ (%) | 81.27 ± 0.70 | 77.29 | 84.04 | 280 | 1.5 |
| | MSE | 0.93 ± 0.016 | 0.88 | 1.02 | 280 | |
| Validation | $R^2$ (%) | 78.28 ± 1.4 | 74.12 | 83.27 | 120 | |
| | MSE | 0.97 ± 0.042 | 0.84 | 1.27 | 120 | |
| Training | $R^2$ (%) | 84.59 ± 0.20 | 83.19 | 86.01 | 422 | 2.0 |
| | MSE | 0.96 ± 0.031 | 0.81 | 1.12 | 422 | |
| Validation | $R^2$ (%) | 81.21 ± 0.76 | 77.57 | 84.21 | 182 | |
| | MSE | 1.11 ± 0.045 | 0.93 | 1.36 | 182 | |
| Training | $R^2$ (%) | 86.95 ± 0.10 | 86.70 | 87.61 | 556 | 2.5 |
| | MSE | 0.58 ± 0.011 | 0.52 | 0.62 | 556 | |
| Validation | $R^2$ (%) | 85.15 ± 0.21 | 84.31 | 86.60 | 239 | |
| | MSE | 0.59 ± 0.013 | 0.52 | 0.66 | 239 | |
| Training | $R^2$ (%) | 81.39 ± 0.62 | 78.10 | 83.01 | 448 | 3.0 |
| | MSE | 1.07 ± 0.012 | 1.02 | 1.16 | 448 | |
| Validation | $R^2$ (%) | 77.33 ± 0.91 | 73.70 | 81.40 | 193 | |
| | MSE | 1.36 ± 0.045 | 1.15 | 1.63 | 193 | |

* Sample size for training and validation

**Table 4 -** Time needed to begin backwashing

| Flow rate ($m^3\ h^{-1}$) | Cleaning time (s) | | | Pressure load (mH2O) |
|---|---|---|---|---|
| | MLP (high) | MLP (low) | Mean | |
| 1.5 | 380 | 540 | 256.20 | 9.0 |
| 2.0 | 200 | 250 | 226.75 | 10.0 |
| 2.5 | 290 | 310 | 293.77 | 11.0 |
| 3.0 | 195 | 188 | 211.28 | 12.0 |

Flow rate ($m^3\ h^{-1}$)

The results for performance when adjusting the artificial neural network for each flow rate can be seen in Table 5.

After some experimentation, different architectures were implemented depending on the test flow rate. For 1.5 $m^3\ h^{-1}$, the topology chosen was the 5-14-2 configuration, i.e. an input layer of dimension p = 5 (4 plus the bias term), a hidden layer with 14 neurons, and an output layer with 2 neurons (pressure load on the filter and filtering time at that load). Architectures of 5-25-2, 5-40-2 and 5-40-2 were modelled for the flow rates of 2.0, 2.5 and 3.0 $m^3\ h^{-1}$. Factors with different characteristics are difficult to generalise using a single MLP (MOON *et al*., 2019), therefore using MLPs with different structures increases the computational complexity but affords greater accuracy (MOON *et al*., 2018).

When it came to estimating the pressure load, the models performed poorly during both the training and validation stages. The average coefficient of determination ranged from 28.76% (flow rate 2.5 $m^3\ h^{-1}$) to 50.28% at a flow rate of 1.5 $m^3\ h^{-1}$ for the training stage. During generalisation, $R^2$ varied between 6.35% (3.0 $m^3\ h^{-1}$) and 30.85% (1.5 $m^3\ h^{-1}$).

On the other hand, the 'time associated with the pressure load' output neuron had the lowest $R^2$ during the training stage at the flow rate of 2.0 $m^3\ h^{-1}$ (26.39%) and the highest (66.64%) at 1.5 $m^3\ h^{-1}$. During validation, the $R^2$ ranged from 6.67% (2.0 $m^3\ h^{-1}$) to 41.43% (1.5 $m^3\ h^{-1}$).

**Table 5** - Performance statistics during the training and validation stages for pressure-load and time adjustment as a function of water quality characteristicss

| Flow rate (1.5 $m^3h^{-1}$) | Pressure load | | | Time | | | |
|---|---|---|---|---|---|---|---|
| Training | Mean | Min. | Max. | Mean | Min. | Max. | n* |
| $R^2$ (%) | 50.28 ± 0.749 | 46.01 | 52.855 | 66.64 ± 1.64 | 60.01 | 73.07 | 300 |
| MSE | 2.47 ± 0.093 | 2.07 | 3.04 | 4640.71 ± 301.03 | 3859.01 | 6542.77 | 300 |
| Validation | | | | | | | |
| $R^2$ (%) | 30.85 ± 1.82 | 20.41 | 43.24 | 41.43 ± 1.77 | 29.72 | 48.26 | 100 |
| MSE | 3.21 ± 0.123 | 2.57 | 4.04 | 7045.29 ± 274.58 | 6269.15 | 8910.19 | 100 |
| Flow rate (2.0 $m^3$ $h^{-1}$) | Pressure load | | | Time | | | |
| Training | Mean | Min. | Max. | Mean | Min. | Max. | n* |
| $R^2$ (%) | 31.45 ± 0.919 | 30.01 | 37.79 | 26.39 ± 1.42 | 19.74 | 31.59 | 345 |
| MSE | 5.15 ± 0.187 | 4.05 | 5.95 | 3288.63 ± 136.38 | 2505.29 | 3727.12 | 345 |
| Validation | | | | | | | |
| $R^2$ (%) | 8.16 ± 1.46 | 2.49 | 19.07 | 6.67 ± 1.28 | 1.48 | 15.28 | 115 |
| MSE | 5.08 ± 0.195 | 4.53 | 6.25 | 3343.38 ± 85.45 | 3002.21 | 3792.54 | 115 |
| Flow rate (2.5 $m^3$ $h^{-1}$) | Pressure load | | | Time | | | |
| Training | Mean | Min. | Max. | Mean | Min. | Max. | n* |
| $R^2$ (%) | 28.76 ± 0.966 | 20.28 | 30.18 | 37.69 ± 3.57 | 16.32 | 55.27 | 480 |
| MSE | 2.94 ± 0.128 | 2.50 | 3.63 | 4692.94 ± 289.53 | 3373.34 | 6064.89 | 480 |
| Validation | | | | | | | |
| $R^2$ (%) | 8.32 ± 1.24 | 2.44 | 15.34 | 7.16 ± 1.46 | 1.07 | 13.31 | 160 |
| MSE | 3.68 ± 0.147 | 2.79 | 4.40 | 6935.47 ± 123.14 | 6290.95 | 7542.722 | 160 |
| Flow rate (3.0 $m^3$ $h^{-1}$) | Pressure load | | | Time | | | |
| Training | Mean | Min. | Max. | Mean | Min. | Max. | n* |
| $R^2$ (%) | 29.46 ± 0.517 | 24.90 | 30.29 | 50.04 ± 3.22 | 33.42 | 64.43 | 480 |
| MSE | 4.48 ± 0.217 | 3.45 | 5.76 | 2397.52 ± 192.88 | 1565.67 | 3595.51 | 480 |
| Validation | | | | | | | |
| $R^2$ (%) | 6.35 ± 0.583 | 3.46 | 8.94 | 19.40 ± 2.21 | 5.74 | 29.29 | 160 |
| MSE | 5.47 ± 0.191 | 4.61 | 6.45 | 3649.32 ± 120.21 | 3045.51 | 4541.72 | 160 |

* Sample size for training and validation

It is important to note that the low accuracy in modelling the pressure load and time via MLP may be associated with the experimental conditions under which the tests were conducted. The volume of solution used (a mixture of humus and water) with a high humus concentration, may have influenced the results, since the 120 mesh (1”) filter had a filtration surface of 100 $cm^2$, which may not have been enough to significantly alter the water quality characteristics.

## CONCLUSIONS

1. Modelling to obtain optimum backwashing thresholds as a function of pressure load performed well using multilayer perceptron feedforward artificial neural networks with a 2-4-1 architecture in a screen filtration system (120 mesh);
2. The models used to adjust the difference in backwash pressure based on water quality characteristics (pH, turbidity, total dissolved solids, and temperature) performed poorly.

## REFERENCES

ADIN, A.; ALON, G. Mechanisms and process parameters of filter screens. **Journal of Irrigation and Drainage Engineering**, v. 112, n. 4, p. 293-304, 1986.

AYERS, R. S.; WESTCOT, D. W. **A qualidade da água na agricultura**. Tradução de: GHEYI, R. S.; MEDEIROS, J. F.; DEMASCENO, F. A.V. Campina Grande: UFPB, 1991. 218 p. (Estudos FAO. Irrigação e Drenagem, 29).

CAMARGO, A. P.; SENTELHAS, P. C. Avaliação do desempenho de diferentes métodos de estimativa da evapotranspiração potencial no Estado de São Paulo. **Revista Brasileira de Agrometeorologia**, v. 5, n. 1, p. 89-97, 1997.

CHI, Y. *et al.* The study on internal flow characteristics of disc filter under different working condition. **Applied Sciences**, v. 11, n. 16, p. 7715-7722, 2021.

DURAN-ROS, M. *et al.* Performance and backwashing efficiency of disc and screen filters in microirrigation systems. **Biosystems Engineering**, v. 1, n. 103, p. 35-42, 2009.

ELBANA, M.; CARTAGENA, F. R.; PUIG-BARGUÉS, J. Effectiveness of sand media filters for removing turbidity and recovering dissolved oxygen from a reclaimed effluent used for micro-irrigation. **Agricultural Water Management**, v. 111, p. 27-33, 2012.

FATHA, A. H.; MADANIFARB, F.; ABBASIA, M. Implementation of multilayer perceptron (MLP) and radial basis function (RBF) neural networks to predict solution gas-oil ratio of crude oil systems. **Petroleum**, v. 6, n. 1, p. 80-91, 2020.

HEMMAT ESFE, M. *et al.* Thermal conductivity of Cu/TiO2–water/EG hybrid nanofluid: experimental data and modeling using artificial neural network and correlation. **International Communications in Heat and Mass Transfer**, v. 66, p. 100-104, 2015.

JIANHUA, L. *et al.* Experimental study on hydraulic performance of hydraulically driven self-cleaning mesh filter [J]. **Yellow River**, v. 41, n. 9, p. 165-172, 2019.

KANNAN, B. *et al.* Development and evaluation of low cost drip filter. **Current Journal of Applied Science and Technology**, v. 39, n. 8, p. 87-94, 2020.

KHAN, T. A.; REHMAN, A. U.; JAMAL, M. N. To investigate the performance of disc filter in retaining clay and sand particles. **International Journal of Scientific Engineering and Applied Science (IJSEAS)**, v. 3, n. 4, p. 87-92, 2017.

LEE, S.; LEE, K.; YOON, H. Using artificial neural network models for groundwater level forecasting and assessment of the relative impacts of influencing factors. **Hydrogeology Journal**, v. 27, n. 2, p. 567-79, 2019.

MESQUITA, M.; TESTEZLAF, R.; RAMIREZ, J. C. S. The effect of media bed characteristics and internal auxiliary elements on sand filter head loss. **Agricultural Water Management**, v. 115, n. 4, p. 178-185, 2012.

MOON, T. *et al.* Interpolation of greenhouse environment data using multilayer perceptron. **Computers and Electronics in Agriculture**, v. 166, p. 105023-105030, 2019.

MOON, T. W. *et al.* Estimation of greenhouse CO2 concentration via an artificial neural network using environmental factors. **Horticulture, Environment and Biotechnology**, v. 59, p. 45-50, 2018.

RIBEIRO, T. A. P. *et al.* Comparison of filtrating elements in the treatment of irrigation water. **Transactions of the ASAE**, v. 51, p. 441-453, 2008.

RIBEIRO, T. A. P. *et al.* Efeito da qualidade da água na perda de carga em filtros utilizados na irrigação localizada. **Revista Brasileira de Engenharia Agrícola e Ambiental**, v. 9, n. 1, p. 1-6, 2005.

SALCEDO, J. C.; TESTEZLAF, R.; MESQUITA, M. Processo de retrolavagem em filtros de areia usados na irrigação localizada. **Engenharia Agrícola**, v. 31, n. 6, p. 1226-1237, 2011.

SOLÉ-TORRES, C. *et al.* Effect of underdrain design, media height and filtration velocity on the performance of microirrigation sand filters using reclaimed effluents. **Biosystems Engineering**, v. 187, p. 292-304, 2019.

TESTEZLAF, R. Filtros de areia aplicados à irrigação localizada: teoria e prática. **Revista Engenharia Agrícola**, v. 28, n. 3, p. 604-613, 2008.

WILLMOTT, C. J. *et al.* Statistics for the evaluation and comparison of models. **Journal of Geophysical Research**, v. 90, n. 5, p. 8995-9005, 1985.

WU, W. *et al.* A new model for head loss assessment of screen filters developed with dimensional analysis in drip irrigation systems. **Irrigation and Drainage**, v. 63, n. 4, p. 523-531, 2014.

ZAKI, M. G. H. *et al.* Evaluation of friction head loss as a function of media filter performance via different underdrain types and media specifications. **CIGR Journal**, v. 23, n. 1, p. 1-11, 2021.

ZONG, O. *et al.* Backwashing performance of self-cleaning screen filters in drip irrigation systems. **Plos One**, v. 14, n. 2, p. 1-18, 2019.

ZONG, Q. *et al.* Development of head loss equations for selfcleaning screen filters in drip irrigation systems using dimensional analysis. **Biosystems Engineering**, v. 133, p. 116-127, 2015.